Supporting information

$MoO_{3-x}NiMoO_4$ nanorods synthesized using NiO nanoparticles for hydrogen evolution in anion exchange membrane water electrolysis

Francesco Bartoli, Carolina Castello, Tailor Peruzzolo, Enrico Berretti, Eva Sediva, Karel Bouzek, Jaromir Hnát, Michaela Plevova, Lorenzo Poggini, Hamish Andrew Miller*

In Figure S1 equivalent electrical circuit used for evaluation of the impedance spectra measured using 78.5 cm^2 electrolysis cell is shown. Used equivalent electrical circuit is literature based and it was used in agreement with previous experience accummulated during studying anion exchange membrane water electrolysis cells.[1,2] Element *L* represents inductance, which is mostly present due to the cables connecting the potentiostat and studied cell. Inductance is typically visible at high frequencies of the perturbing signal.

Value *Rs* stands for ohmic resistance of the measured system, including resistance of the connecting cables, current feeders, electrodes and electrode compartments separator. In the well constructed cell, the main contributor to this quantity represents the electrode compartments separator. The *Rs* value corresponds to the Z''=0 at high frequencies of the perturbing signal.

Values *Rp1* and *Rp2* correspond to polarisation resistances, which are related to the charge transfer through the electrolyte|electrode boundary. *Rp1* and *Rp2* are thus directly related to the kinetic of the anode and cathode reaction respectively. In the case of one electrode reaction (anodic oxygen or cathodic hydrogen evoluiton respectively) is significantly slower than the second one, the equivalent electrical circuit can be simplified neglecting the values *Rp2* and *CPE2* representing the faster reaction. This is the case of $NiCo_2O_4$ used on anode side. *CPE1* and *CPE2* are constat-phase elements. CPE represents capacitor with distributed value of capacity. It is typically used to characterise the 3D electrodes. Value of CPE thus describes the capacity of the electric double layer of the electrolyte|electrode boundary.

Value *Rpor* describes resistivity of the electrolyte filling pores of the 3D electrode. Correspondingly, value C1 is also connected with capacity of the electric double layer on the 3D electrode pore walls.

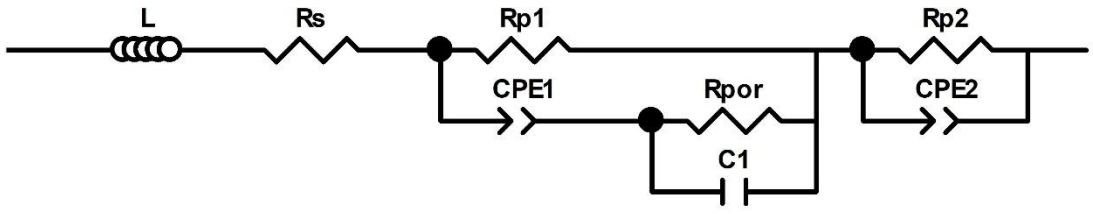

Figure S1: The equivalent circuit used for evaluation of EIS measured using 78.5 cm^2 cell. *L* [H] (inductance of connecting cables), *Rs* [Ω] (system resistivity), *Rp1* and *Rp2* [Ω] (polarisation resistance), *CPE1&2* [F s^{n-1}, where n represents frequency dispersion with the range of 0 to 1] (constant phase element), *Rpor* [Ω] (resistance of liquid electrolyte in Ni foam pores), *C1* [F] (capacity of the double layer on the pore walls of the Ni foam).

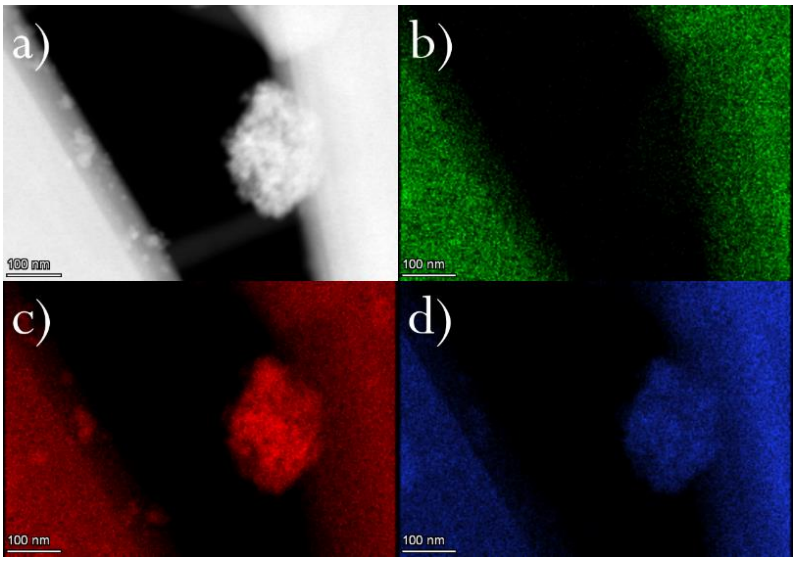

Figure S2: STEM images and elemental mapping of $NiMoO_4$ precursor b) Mo, c) Ni, d) O.

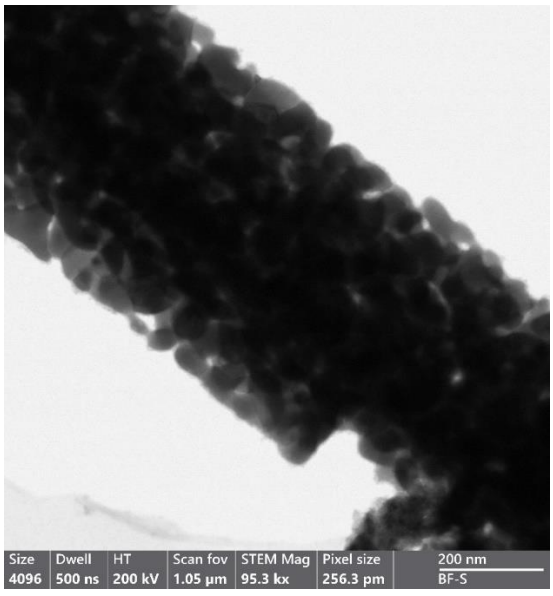

Figure S3: TEM micrograph (bright field) of $MoO_{3-x}NiMoO_4$ (600 °C).

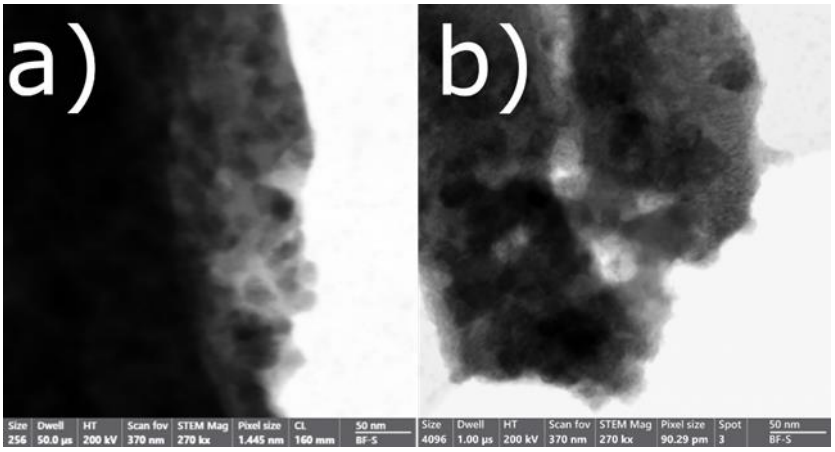

Figure S4*:* TEM bright field of $MoO_{3-x}NiMoO_4$ a) 500 °C and b) 600 °C.

Table S1: Elemental $NiMoO_4$ composition obtained by XPS

	Mo	Ni	O
Element Percentage	9.3%	9.6%	81.2%
Experimental stoichiometry [a]	1	0.7	4.4

[a] Experimental stoichiometry normalised to Mo.

	Mo/Ni	Ni/Mo	Mo/O	Ni/O	Mo+Ni/O
Experimental elements ratio	0.97	1.03	0.11	0.12	0.23

Table S2: Elemental $MoO_{3-x}NiMoO_4$ (500 °C) composition obtained by XPS

	Mo	Ni	O
Element Percentage	10.1%	2.4%	88.74%
Experimental stoichiometry [a]	1	0.2	4.3

[a] Experimental stoichiometry normalised to Mo

	Mo/Ni	Ni/Mo	Mo/O	Ni/O	Mo+Ni/O
Experimental elements ratio	4.15	0.24	0.12	0.03	0.14

Table S3: Elemental $MoO_{3-x}NiMoO_4$ (600 °C) composition obtained by XPS

	Mo	Ni	O
Element Percentage	10.9%	5.0%	84.1%
Experimental stoichiometry [a]	1	0.3	3.8

[a] Experimental stoichiometry normalised to Mo

	Mo/Ni	Ni/Mo	Mo/O	Ni/O	Mo+Ni/O
Experimental elements ratio	2.20	0.45	0.13	0.06	0.19

Table S4: composition (%) relative to the different oxidation states of Mo by XPS.

	Mo (0) %	**Mo (IV) %**	**Mo (V) %**	**Mo (VI) %**
$NiMoO_4/Ni_{foam}$ (previous work)	2.6	28	8.3	61
$NiMoO_4$	-	-	4	-
MoO_2/Ni_{foam} 500 °C (previous work)	22.2	57.9	16.5	3.4
$MoO_{3-x}NiMoO_4$ (500 °C)	0	7	35	58
MoO_2/Ni_{foam} 600°C (previous work)	17.1	65.9	13.9	3.1
$MoO_{3-x}NiMoO_4$ (600 °C)	1	36	9	54

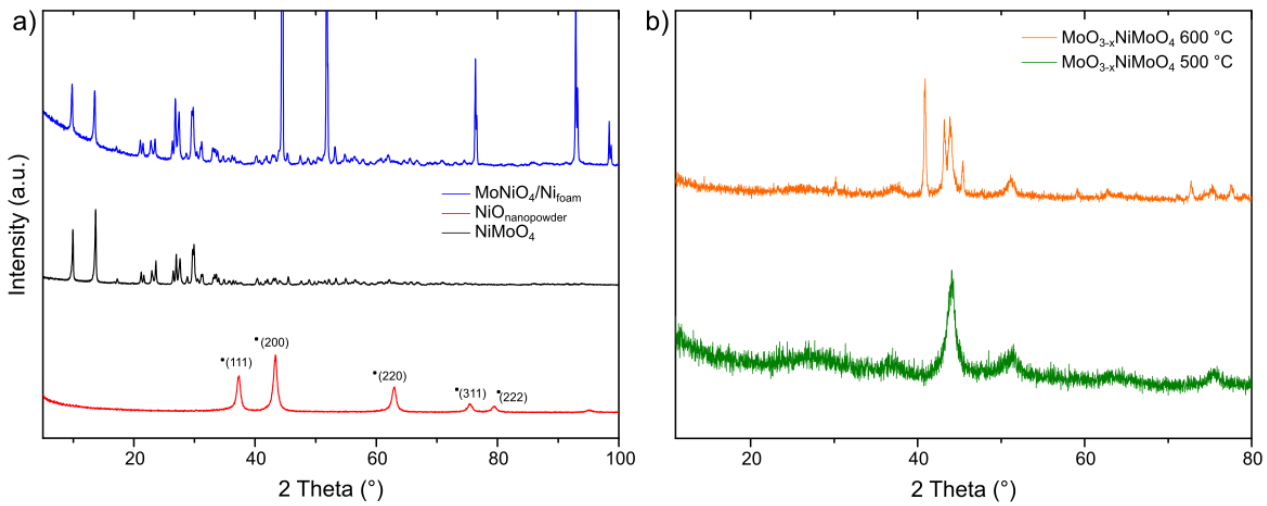

Figure S5: a) Comparison of bare NiO nanopowder [3] then $MoNiO_4$ precursor grown onto NiO and $MoNiO_4$/Ni foam from previous work [4]. b) Comparison spectra of $MoO_{3-x}NiMoO_4$ 500 °C and $MoO_{3-x}NiMoO_4$ 600 °.

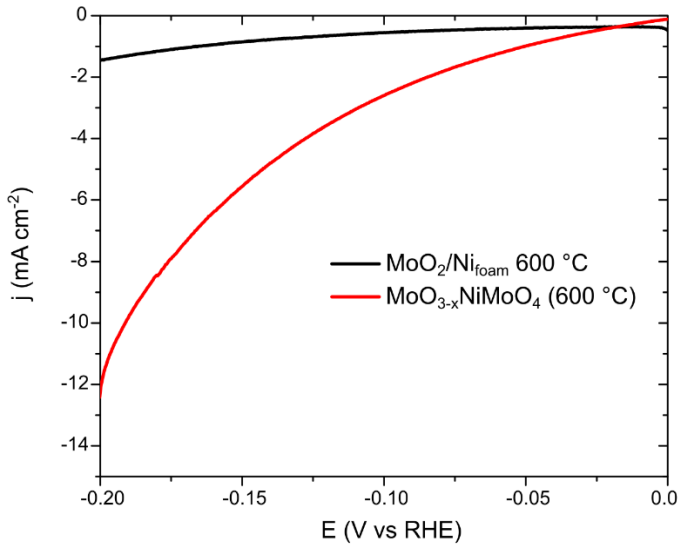

Figure S6: Comparison between MoO_2/Ni_{foam} 600 °C (previous work) and $MoO_{3-x}NiMoO_4$ (600 °C). LSV registered at 1 mV s^{-1} @ 1600 rpm, 0.1 M KOH.

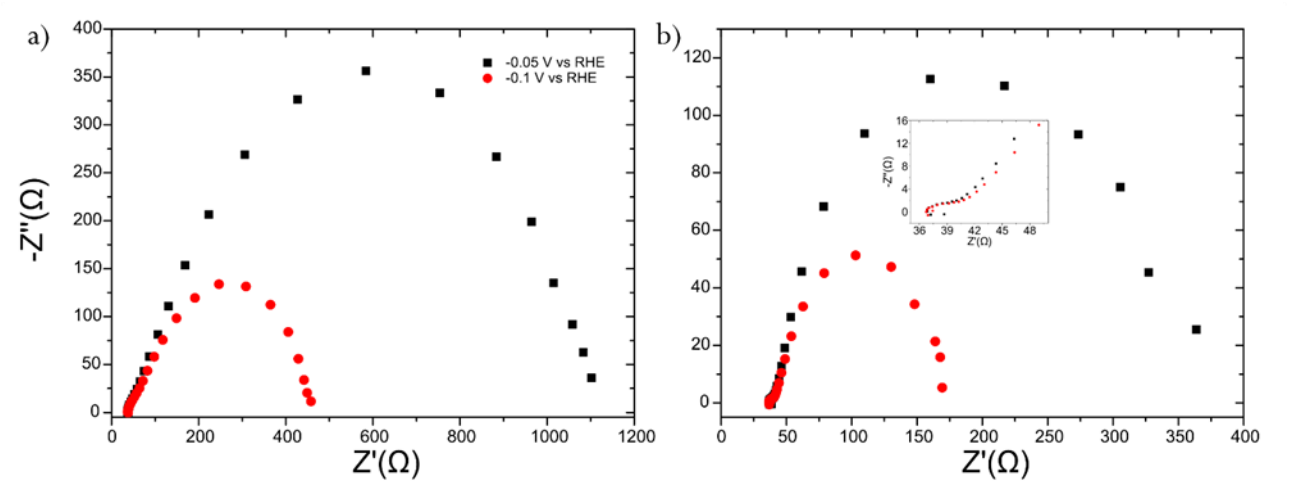

Figure S7: Nyquist plot for a) $MoO_{3-x}NiMoO_4$ (500 °C) and b) $MoO_{3-x}NiMoO_4$ (600 °C), recorded at different potentials.

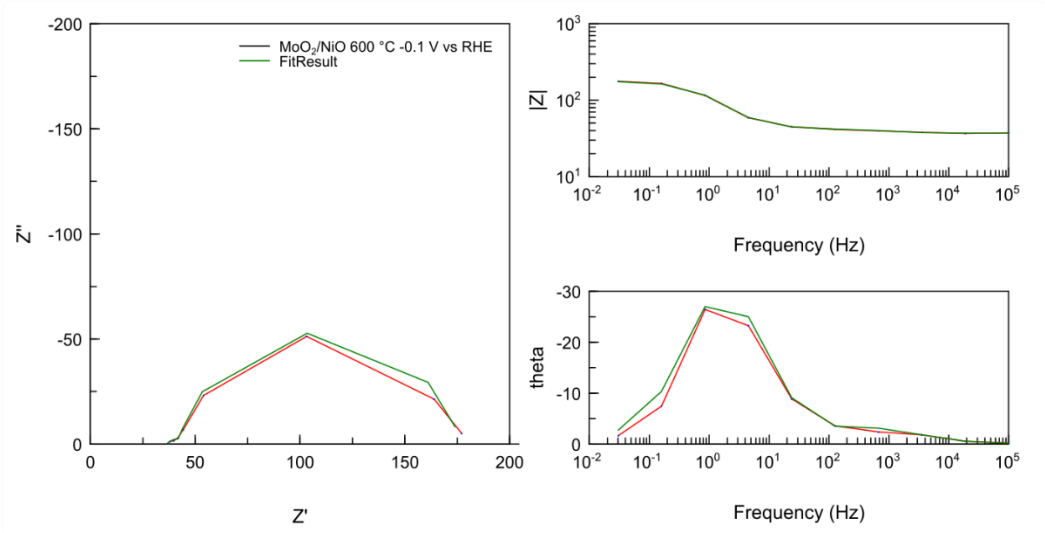

Figure S8: fit results for $MoO_{3-x}NiMoO_4$ (600 °C) at -0.1 V vs RHE.

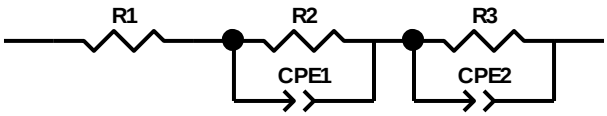

Element	Freedom	Value	Error	Error %
R1	Fixed(X)	37	N/A	N/A
R2	Fixed(X)	4,9	N/A	N/A
CPE1-T	Fixed(X)	0,0002551	N/A	N/A
CPE1-P	Fixed(X)	0,8	N/A	N/A
R3	Free(+)	134,5	2,4759	1,8408
CPE2-T	Free(+)	0,0019835	8,9794E-05	4,527
CPE2-P	Free(+)	0,84953	0,01467	1,7268

Figure S9: Equivalent circuit for $MoO_{3-x}NiMoO_4$ (600 °C) at -0.1 V vs RHE with relative circuital elements values.

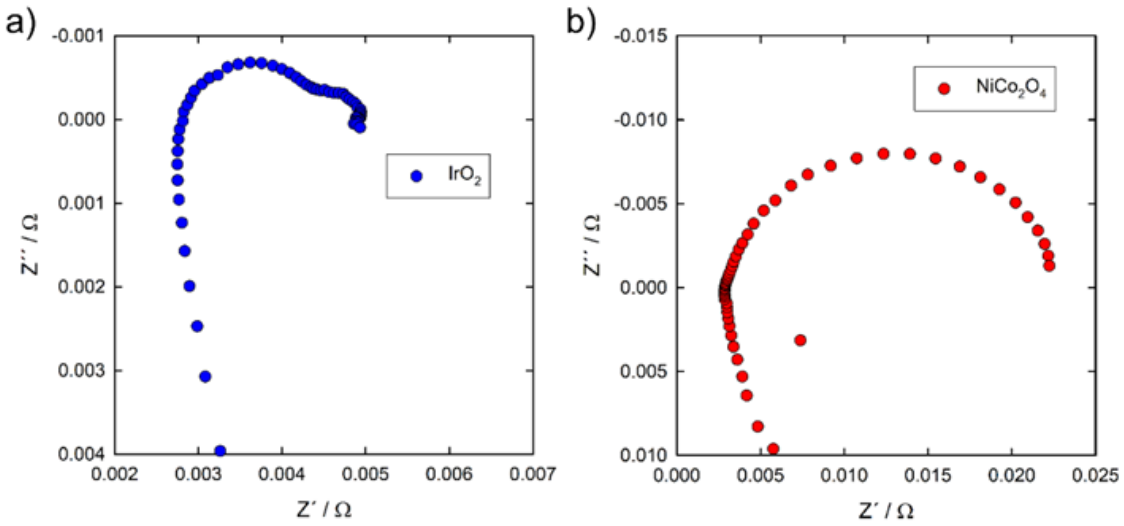

Figure S10: Nyquist plots of the EIS measurements using the $MoO_{3-x}NiMoO_4$ 600 °C cathode and anodes with IrO_2 or $NiCo_2O_4$ catalysts respectively. EIS measured in the frequency range 100 kHz–10Hz, with maximal amplitude 10 mV at cell voltage 1.6 V

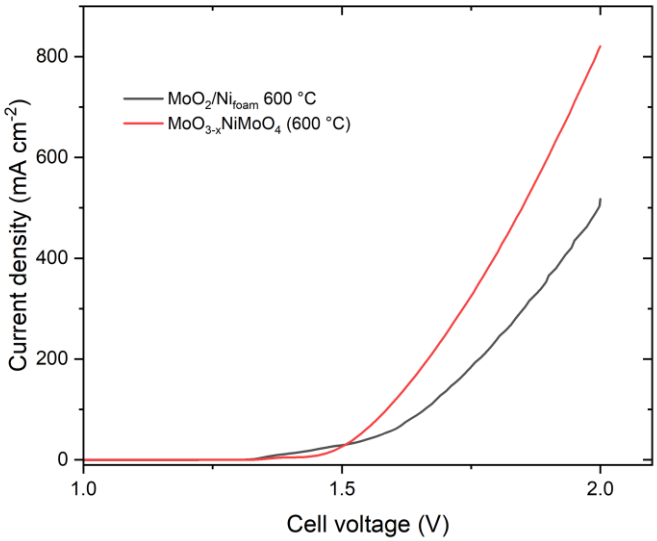

Figure S11: Comparison between MoO_2/Ni_{foam} 600 °C (previous work) and $MoO_{3-x}NiMoO_4$ (600 °C). Cell test performed with Ni foam anode at 60 °C, 1 M KOH feed to the anode.

Table S5: comparison of different electrocatalysts for HER at -10 mA cm^{-2}.

Electrocatalyst	Overpotential (mV)	Electrolyte	Ref.
Ni-MoO_2 /NF	38.3	KOH 1 M	5
Ti@$Ni(OH)_2$-NiMoS	180	KOH 1 M	6
Ni/MoO_{2-x} @NF	27	KOH 1 M	7
MoNi/$NiMoO_x$	9	KOH 1 M	8
NiMoN	20	KOH 1 M	9
NiMo@ZnO/NF	110	KOH 1 M	10
QAMN	240	KOH 0.1 M	11
$MoO_{3-x}NiMoO_4$ 600 °C	190	KOH 0.1 M	This work

Table S6: Performance comparison of literature AEMWE data with Ni-Mo cathodes

Anion Exchange Membrane	**Anion Exchange Ionomer**	**Cathode Catalyst**	**Anode catalyst**	**Electrolyte**	**Cell temp. °C**	**A cm^{-2} @ Vcell**	**Durability data**	**Ref.**
FAA-3-PK-130	Fumasep FAA-3-film	MoO3-xNiMoO4 (600 °C)	Ni foam	1 M KOH @ anode	60	0.82 @2	50 h 1 A cm^{-2}	this work
FAA-3-PK-130	--	MoO_2/Ni	Fe-MoNi/Ni	1 M KOH @anode	60	0.55 @2	300 h 0.5 A cm^{-2}	previous work [4]
FAA-3-PK-130	Fumasep FAA-3-film	$MoO_{3-x}NiMoO_4$ (600 °C)	IrO2	1 M KOH	50	0.9@1.8		this work
FAA-3-PK-130	Fumasep FAA-3-film	$MoO_{3-x}NiMoO_4$ (600 °C)	NiCoO4	1 M KOH	50	1.0@2.0		this work
PTFE-Sustainion	Nafion	Ni-Mo	Fe-Ni-Mo	1 M KOH @cathode	80	1.0 @1.57	--	[12]
FAA-3–50	FAA3	$NiMo/K^B$	NiFe (85:15 at.%)	1 M KOH @anode	50	1.0 @1.8	2000 h 1 A cm^{-2}	[13]
PVBC-MPy/35%PEK-cardo	--	Ni-Mo	Ni-Fe	1 M KOH	60	0.5 @2	42 h 0.5 A cm^{-2}	[14]
FAA-3-PK-130	--	$MoNi/NiMoO_x$	$Co_2(OH)_3Cl$/ FeOOH	1 M KOH	25	0.5 @ 3.05	1600 h 0.2 A cm^{-2}	[8]
Sustainion® X37-50	--	NiMo/TP-4	NiFe/TP-4	1 M KOH	50	--	100 h 1 A cm^{-2}	[15]
PFTP-13	--	20 mg cm^{-2} Ni–Fe	20 mg cm^{-2} Ni–Fe	1 M KOH cathode	80	1.6 @2.0	1000 h, 0.5 A cm^{-2}, 60 C, no degr	[16]

References:

[1] C. Hitz, A. Lasia, Journal of Electroanalytical Chemistry, 2001, 500, Issues 1–2, 213.

[2] G. Schiwietz, P.L. Grande, Nuclear Instruments and Methods in Physics Research Section B: Beam Interactions with Materials and Atoms, 2001, 175–177, 125.

[3] Z. Wei, H. Qiao, H. Yang C. Zhang X. Yan, Journal of Alloys and Compounds 2009, 479, 855.

[4] F. Bartoli, L. Capozzoli, T. Peruzzolo, M. Marelli, C. Evangelisti, K. Bouzek, J. Hnát, G. Serrano, L. Poggini, K. Stojanovski, V. Briega-Martos, S. Cherevko, H. A. Miller, F. Vizza, *J Mater Chem A Mater* 2023, DOI 10.1039/D2TA09339A.

[5] J.-T. Ren, L. Wang, L. Chen, X.-L. Song, Q.-H. Kong, H.-Y. Wang, Z.-Y. Yuan, Small, 2023, 19, 5, 2206196.

[6] Yang C, Zhou L, Yan T, Bian Y, Hu Y, Wang C, Zhang Y, Shi Y, Wang D, Zhen Y, Fu F. J Colloid Interface Sci. 2022 Jan 15;606(Pt 2):1004-1013.

[7] Wanli Liang, Mengyan Zhou, Xiulan Li, Lijie Zhu, Zhixin Li, Yifan Zhou, Jian Chen, Fangyan Xie, Hao-Fan Wang, Nan Wang, Yanshuo Jin, Hui Meng, Chemical Engineering Journal, 464, 2023, 142671.

[8] X. Shi, X. Zheng, H. Wang, H. Zhang, M. Qin, B. Lin, M.i Qi, S. Mao, H. Ning, R.Yang, L. Xi, Y. Wang. Adv. Funct. Mater. 2023, 33, 2307109

[9] Liuyu Jia, Jing Li, Xiaorui Yu, Lizhi Feng, Liu Yang, Yiyan Yang, Wenfeng Ye, and Baodan Liu ACS Applied Nano Materials 2023 6 (2), 1050-1058

[10] Jun Cao, Haichao Li, Ruitong Zhu, Li Ma, Kechao Zhou, Qiuping Wei, Fenghua Luo, Journal of Alloys and Compounds, Volume 844,2020,155382,

[11] Doudou Zhang, Jingying Shi,* Yu Qi, Xiaomei Wang, Hong Wang, Mingrun Li,Shengzhong Liu,* and Can Li Adv. Sci. 2018, 5, 1801216

[12] P. Chen, X. Hu, *Adv Energy Mater* 2020, *10*, 2002285.

[13] S. Campagna Zignani, M. Lo Faro, A. Carbone, C. Italiano, S. Trocino, G. Monforte, A. S. Aricò, *Electrochim Acta* 2022, *413*, 140078.

[14] H. Li, M. R. Kraglund, A. K. Reumert, X. Ren, D. Aili, J. Yang, *J Mater Chem A Mater* 2019, *7*, 17914.

[15] J. Hyun Oh, G. Ho Han, J. Kim, J. Eun Lee, H. Kim, S. Kyung Kang, H. Kim, S. Wooh, P. Soo Lee, H. Won Jang, S. Young Kim, S. Hyun Ahn, *Chemical Engineering Journal* 2023, *460*, 141727.

[16] N. Chen, S. Y. Paek, J. Y. Lee, J. H. Park, S. Y. Lee, Y. M. Lee, *Energy Environ Sci* 2021, *14*, 6338.